DOE/FETC/C--98/7303
CONF-9704176--

THE EFFECT OF PRESSURE ON SOLID OXIDE FUEL CELL PERFORMANCE

Anil V. Virkar and Kuan-Zong Fung
Department of Matl's. Sci. & Engr., 304 EMRO
University of Utah
Salt Lake City, UT 84112

and

Subhash C. Singhal
Westinghouse Electric Corporation
1310 Beulah Road
Pittsburgh, PA 15235

ABSTRACT

Current work in solid oxide fuel cells (SOFCs) is on cathode-supported, anode-supported, or electrolyte-supported cells. In electrode-supported cells, a thin film (5 to 30 μm) of an electrolyte (YSZ) is deposited on a relatively thick, porous electrode. In electrolyte-supported cells, the electrolyte thickness is typically ≥ 150 μm upon which thin electrodes are screen-printed. Both types of SOFCs are being explored for hybrid applications, that is in combination with a gas turbine, for which the exit gases from an SOFC generator must be at a high pressure (3 to 15 atm) for input into a gas turbine. It is necessary to examine the expected performance of an SOFC under a high pressure. Work at Westinghouse/Ontario Hydro has shown that the performance improvement at high pressures is greater than that can be expected based on an increased Nernst potential alone. This increased performance can in part be attributed to a lower concentration polarization. The objective of this work was to conduct a preliminary analysis of the effect of pressure on the performance of both cathode-supported and electrolyte-supported cells. Flux equations for transport through porous electrodes are formulated and are solved in combination with those for electrochemical operation of an SOFC for cathode-supported and electrolyte-supported cells. The analysis shows that the overall cell performance increases significantly with increasing pressure in the case of cathode-supported cells due to a lowering of concentration polarization at high pressures. Similar effects (not presented here) are also observed on anode-supported cells. By contrast, only a modest improvement is observed in the case of electrolyte-supported cells, commensurate with the fact that in latter, the ohmic contribution of the electrolyte is the most dominant one, which is not altered by pressure.

I. INTRODUCTION

Electrochemical conversion of chemical energy of a fuel into electrical energy by fuel cells continues to be an important thrust area of energy conversion technology [1]. Among these, high temperature fuel cells using either a molten salt or solid oxide electrolytes are of particular interest. This is because operation at higher temperatures allows for the use of natural gas as a fuel unlike low temperature PAFC or PEM fuel cells

DISCLAIMER

which must use hydrogen to prevent electrode poisoning due to carbon monoxide. The high temperature fuel cells are of two types: molten carbonate fuel cells (MCFC) and solid oxide fuel cells (SOFC). Considerable effort is currently directed towards both types of high temperature fuel cells for stationary power generation. The overall system efficiency can be significantly increased using a hybrid concept involving a combination of high temperature fuel cell generator and a gas turbine [2]. The best operating conditions for a hybrid cycle require high operating temperatures ($\geq$ 800°C) and pressures greater than one atmosphere (typically 3 to 15 atm.) [3]. Operation at pressures greater than one atmosphere, and possibly approaching 15 atmospheres, leads to SOFC as the clear choice since issues regarding materials instability at elevated temperatures become a critical limitation for the MCFC system. The following discussion is thus confined to the SOFC. Higher operating temperatures for a hybrid application may appear to be a step in an opposite direction to the recent trend which seeks to lower the operating temperature of an SOFC, typically below 800°C. Thus, it is to be mentioned at the outset that recent efforts directed towards lowering the cell operating temperature while still maintaining a high power density are also relevant to the higher temperature operation since even higher power densities are possible at elevated temperatures using these high performance cells. It is to be emphasized that the attainment of as high a power density as possible is clearly desired since it means the attainment of as low a cell (area specific) resistance as possible. The lower the cell resistance, the lower is the heat generation due to internal heating for a given current or a given power output. Thus, thermal management, in principle, is less of an issue with high performance cells.

Westinghouse has reported work on the pressurized operation of its tubular SOFCs [3-5]. The SOFCs were operated at pressures as high as 15 atmospheres, i.e., both the fuel and the oxidant at high but equal pressures such that there is no pressure differential across the tubes. The increase in pressure does not alter the partial pressure of oxygen (pO_2) on the anode side since the pO_2 depends upon the ratio pH_2O/pH_2 (or on pCO_2/pCO) which is independent of the net pressure of the anodic gases. However, the pO_2 at the cathode is directly proportional to the total pressure of the cathodic gas (which is air). The Nernst potential is given by

$$E = \frac{RT}{4F} \ln\left(\frac{p_{O_{2(o/c)}}}{p_{O_{2(o/a)}}}\right) \qquad (1)$$

Thus, an increase in pressure from 1 atm to 10 atm at 1000°C will lead to an increase in the Nernst potential of ~63 mV and an increase of ~53 mV at 800°C. The corresponding increase in the maximum power density based on this should be approximately 13% at 1000°C and ~10% at 800°C. It was observed in the Westinghouse work, however, that the increase in cell performance was greater than can be rationalized on the basis of improvement in the Nernst potential alone. This increase can be attributed in part to a decrease in concentration polarization. As will be discussed later, an increase in pressure is also expected to lower the activation overpotential. Thus, the beneficial effect of an increase in pressure may be due to two reasons: (1) Decrease in concentration polarization, (2) Decrease in activation polarization. This indeed is a welcome result for hybrid applications. But additionally, this is also important from the standpoint of cell

design as will be discussed below.

Electrode Structure: The indirect observation that polarization losses can be reduced significantly by an increase in pressure suggests that electrode structure must have a profound effect on SOFC performance and further improvements in cell (and thus stack) performance may be realized through a judicious design of electrodes. The Westinghouse work has examined the effect of pressure on cathode-supported tubular SOFCs [3-5]. This manuscript presents preliminary results of calculations which attempt to rationalize the observed improved performance of cathode-supported cells and compares it with expected behavior of an electrolyte-supported cells.

Figure #1 shows schematics of cathode-supported and electrolyte-supported cells. In the former, typical of the Westinghouse design, the cathode thickness is on the order of 2 mm while the electrolyte thickness is ≈ 20 to 30 μm. In the electrolyte-supported cells, the electrolyte thickness is typically on the order of 150 μm or greater, while the electrode (cathode and anode) thicknesses typically are on the order of 25 to 50 μm. In the former, there is potential for significant concentration polarization due to a thick cathode. On the other hand, in the electrolyte-supported cells, the principal limitation on cell performance is due to ohmic losses in the electrolyte itself. The overall performance of a cell can be determined by analyzing transport processes through the porous electrodes (concentration polarization), across electrode/electrolyte interfaces (activation polarization), and through the electrolyte (ohmic polarization) under steady state conditions. The following is a simplified analysis for the case where the activation polarization is ignored. Alternatively, assuming that activation polarization (charge transfer) is confined to a small region of an electrode in contact with the electrolyte, the following tacitly assumes that this contribution is lumped along with the electrolyte contribution itself.

II. ANALYSIS OF TRANSPORT PROCESSES THROUGH THE ELECTRODES

The analysis presented here is based on the following assumptions: (1) Mass transport through the electrodes occurs by diffusion where transport of a given species occurs down its pressure gradient. Also, the analysis ignores the fluxes due to the net pressure gradient, since this effect is expected to be small. (2) There is no charge transfer resistance at the electrode/electrolyte interface. The following terminology will be used:
l_a: Anode thickness (cm), $V_v(a)$: Volume fraction of porosity in the anode
l_c: Cathode thickness (cm), $V_v(c)$: Volume fraction of porosity in the cathode,
l_i: Electrolyte thickness (cm), ρ_i: Electrolyte resistivity (Ωcm)
R_i: Electrolyte specific resistance ($\rho_i l_i$) (Ωcm^2), R_L: Area specific load (Ωcm^2)
$p_{H2(0)}$: Partial pressure of hydrogen in the anode gas (outside of the anode)
$p_{H2O(0)}$: Partial pressure of water vapor in the anode gas (outside of the anode)
$p_{O2(0/c)}$: Partial pressure of oxygen in the cathode gas (outside of the cathode)
$p_{O2(0/a)}$: Partial pressure of oxygen in the anode gas (outside of the anode)
$p_{H2(a)}$: Partial pressure of hydrogen in the anode gas at the anode/electrolyte interface
$p_{H2O(a)}$: Partial pressure of water vapor in the anode gas at the anode/electrolyte interface

$p_{O2(a)}$: Partial pressure of oxygen in the anode gas at the anode/electrolyte interface
$p_{O2(c)}$: Partial pressure of oxygen in the cathode gas at the cathode/electrolyte interface
K_{eq}: Equilibrium constant for the reaction $H_2(g) + {}^1/_2O_2(g) \rightarrow H_2O(g)$
J_{H2}: Flux of hydrogen gas through the anode (#/cm^{2}sec)
J_{H2O}: Flux of water vapor through the anode (#/cm^{2}sec)
J_{O2}: Flux of oxygen through the cathode (#/cm^{2}sec)
i: Current density (amps/cm^2), T: Temperature (°K)
R: Gas constant (j/mol.°K), k_B: Boltzmann constant (ergs/°K), N: Avogadro's number
F: Faraday constant (coulombs/mol), E_o: Nernst potential (volts)

Two types of Nernst potentials are defined here; static and dynamic. The static Nernst potential is the open circuit potential and is given by

$$E_o(s) = \frac{RT}{4F}\ln\left\{\frac{p_{O_2(0/c)}}{p_{O_2(o/a)}}\right\} = \frac{RT}{2F}\ln K_{eq} + \frac{RT}{4F}\ln\left\{\frac{p_{O_2(0/c)}p^2_{H_2(0)}}{p^2_{H_2O(0)}}\right\} \qquad (2)$$

and the dynamic Nernst potential, which is the Nernst potential under an applied load such that a nonzero current flows through the circuit.

The net reaction occurs with the following steps established: (i) A flux of hydrogen through the anode towards the anode/electrolyte interface, (ii) A flux of oxygen through the cathode towards the cathode/electrolyte interface, (iii) A flux (current) of oxygen ions through the electrolyte from the cathode to the anode, (iv) A reaction between hydrogen and oxygen ions to form water vapor and release electrons which transport through the outer circuit (through the load) from the anode to the cathode, and (v) A flux of water vapor from the anode/electrolyte interface through the anode towards the incoming fuel gas. In steady state, the current density through the electrolyte must also be consistent with the fluxes of the various gaseous species through the electrodes. It is easily seen that

$$\frac{iN}{2F} = 2J_{O_2} = J_{H_2O} = J_{H_2} \qquad (3)$$

The current density, i, is given by

$$i = \frac{E_o(d)}{(R_i + R_L)} = \frac{RT}{4F(R_i + R_L)}\ln\left\{\frac{p_{O_2(c)}}{p_{O_2(a)}}\right\} \qquad (4)$$

Once the current density is determined as a function of the various parameters in addition to the load R_L, the corresponding voltage is given by $V = iR_L$ and the power density is given by i^2R_L. Determination of the current density requires the knowledge of $p_{O2(c)}$ and $p_{O2(a)}$, the partial pressures of oxygen at the electrolyte/cathode interface and electrolyte/anode interface, respectively. This, in turn requires a solution to the flux equations (3). Solution to the flux equations necessitates first a formulation of the flux equations. This is briefly described in what follows.

<u>The Effect of Pressure on Cell Performance:</u> Preliminary theoretical analysis of SOFC performance as a function of total pressure has been recently carried out [6]. The analysis is based on explicitly evaluating the effect of pressure on concentration polarization by analyzing gas transport through porous electrodes. The fundamental equations governing the transport of gaseous species through porous electrodes for a

mixture of two gases, A and B, are given by [7]

$$J_A = -D_A \nabla n_A + X_A \delta_A J - X_A \gamma_A \left(\frac{nB_o}{\eta} \right) \nabla p$$

$$J_B = -D_B \nabla n_B + X_B \delta_B J - X_B \gamma_B \left(\frac{nB_o}{\eta} \right) \nabla p \qquad (5)$$

where

$$\frac{1}{D_A} = \frac{1}{D_{AK}} + \frac{1}{D_{AB}} \qquad \delta_A = \frac{D_{AK}}{D_{AK} + D_{AB}} \qquad \gamma_A = \frac{D_{AB}}{D_{AK} + D_{AB}}$$

$$\frac{1}{D_B} = \frac{1}{D_{BK}} + \frac{1}{D_{AB}} \qquad \delta_B = \frac{D_{BK}}{D_{BK} + D_{AB}} \qquad \gamma_B = \frac{D_{AB}}{D_{BK} + D_{AB}} \qquad (6)$$

In the above equations D_{AB} is the binary diffusion, $D_{AK} \& D_{BK}$ are Knudsen diffusivities, $n_A \& n_B$ are the concentrations (#/cm^3), $n = (n_A + n_B)$, $X_A \& X_B$ are the mole fractions, B_o is the permeability, η is the viscosity, p is the total pressure, and J is the total flux. Parameters $\delta_A \& \delta_B$, and $\gamma_A \& \gamma_B$ are as defined above. Equations (5) and (6) include two contributions to the fluxes; a diffusive flux and a viscous flow. The diffusive contribution consists of two (series) terms; free molecule or Knudsen flow (defined by terms containing $D_{AK} \& D_{BK}$), and continuum part. Typical total pressure on the anodic and cathodic sides is on the order of 1 atm or greater. Thus, the contribution of Knudsen flow can be ignored. That is, for high pressures, such as those of interest here, both $D_A \& D_B$ approach D_{AB}, the binary diffusion coefficient, and $\delta_A \& \delta_B \rightarrow 1$, and $\gamma_A \& \gamma_B \rightarrow 0$. Thus, the main contribution to the total flux is continuum diffusion. For the cathode, the D_{AB} refers to the binary diffusion for a mixture of oxygen, O_2, and nitrogen, N_2. Since the molecular weights of oxygen and nitrogen are similar (32 for O_2 and 28 for N_2), error introduced by using oxygen diffusivity as calculated from the kinetic theory of gases is small. On the anode side, the requisite binary diffusion coefficient is that for H_2 and H_2O. Experimental measurements of binary diffusion coefficients for various gas pairs are available at 1 atm pressure at selected temperatures. The dependence of the diffusion coefficient on temperature is not very strong and to a first approximation it may be modified assuming the kinetic theory of gases to be applicable. At room temperature, $D_{O_2-N_2} \approx 0.22$ cm^2/sec and $D_{H_2-H_2O} \approx 0.91$ cm^2/sec. [8]. This demonstrates that concentration polarization effects in general are expected to be less on the anodic side. Finally, the binary diffusion coefficient, D_{AB} must be multiplied by the volume fraction of porosity and divided by the tortuosity factor, τ. The porosity can be easily measured but tortuosity factor is not easily measured. Usually, the tortuosity factor, τ, varies between 2 and 6 for most porous bodies [8]. Since τ is usually not known, it is often necessary to choose some value which gives a good fit between experiments and theory. As the present manuscript primarily gives results on calculations without a direct comparison with experimental data, the tortuosity factor will be assumed to be unity. This will undoubtedly lead to high values of the current densities. Nevertheless, it will provide useful information on predicted trends which can be compared with Westinghouse

results. In what follows, results of calculations on cathode-supported and electrolyte-supported cells are given.

The above equations were solved in combination with those for electrochemical performance [9] to determine the expected voltage vs. current density and power density vs. current density traces. Figure #2 shows calculations for cathode-supported cells for the set of parameters given in the figure caption. Note that power density increases with increasing pressure. For the set of parameters given, note that the maximum power density increases from ~0.25 W/cm^2 at 1 atm to ~1.6 W/cm^2, over a six-fold increase. Obviously, such a drastic improvement is not experimentally observed. There are three reasons for this: (1) The actual current path in the tubular cells is rather long. Consequently, the ohmic contribution is larger than assumed here. (2) Charge transfer (activation polarization) was assumed to be negligible in the calculations. Such may not be the case. (3) The tortuosity factor was assumed to be unity. In reality, it is expected to be significantly greater than unity. The calculations, nevertheless show the level of improvement that can be realized if these losses can be minimized. Recent experimental work has shown that through appropriate electrode designs, charge transfer resistance can be reduced to a value below about 0.15 Ωcm^2. In such cells, a greater effect of pressure is expected, commensurate with calculations.

The corresponding calculated voltage vs. current density traces are also shown in the figure. Although not obvious in the voltage vs. current density traces, the slopes actually decrease with increasing pressure. The slope in the present calculations contains two terms; the ohmic contribution of the electrolyte (which is not affected by pressure) and concentration polarization (which is dependent on pressure). Figure #3 shows a plot of the calculated area specific resistance vs. the net pressure. The pressure dependence of the area specific resistance, over the range of pressures explored, can be adequately given by

$$R_{Cell} \approx 0.0997 + \frac{0.2063}{P} \quad \Omega\text{cm}^2 \qquad (7)$$

The intercept gives the cell resistance at (hypothetically) infinite pressure for which the contribution of concentration polarization should be zero. Thus, the intercept should correspond to the area specific resistance of the electrolyte. For a YSZ thickness of 20 μm with resistivity of 50 Ωcm, the area specific resistance is 0.1 Ωcm^2, very close to the intercept of 0.0997 Ωcm^2.

Similar calculations were performed on electrolyte-supported cells for the following parameters: Electrolyte thickness = 150 μm (which is typical of the thickness used in such SOFCs[10-12]), cathode thickness = 25 μm, and anode thickness = 25 μm, all other parameters being the same. Figure #4 shows calculations for the electrolyte-supported cells. Note that power density increases with increasing pressure. However, the maximum power density exhibits only a modest increase from about ~0.38 W/cm^2 at 1 atm. pressure to ~0.45 W/cm^2 at 10 atm. pressure, in accord with expectations. Area specific resistances obtained from voltage vs. current density traces are also plotted vs. 1/pressure in Figure #3. The area specific resistance can be adequately described by

$$R_{Cell} \approx 0.7526 + \frac{0.029}{P} \ \Omega cm^2 \qquad (8)$$

The calculated area specific resistance of the electrolyte (150 μm thickness) is 0.75 Ωcm^2, close to the intercept of 0.7526 Ωcm^2. The slope of the plot is 0.029 Ωcm^2.atm. while that for the cathode-supported cell is 0.2063 Ωcm^2.atm., about seven times greater consistent with the significant effect of pressure on cell performance.

Comparison with Experimental Observations: No experimental work has been conducted at 800°C and for the conditions assumed in the present calculations. However, as mentioned earlier, work at Westinghouse/Ontario Hydro has shown that there indeed is an improvement which is greater than that can be rationalized on the basis of Nernst potential alone. The work at Westinghouse/Ontario Hydro examined the effect of pressure over a range between 1 and 15 atm. and at 1000°C [3]. Figure #5 shows voltage vs. current density traces at 1000°C over a range of pressures between 1 and 15 atm [3]. The voltage vs. current density traces exhibit a substantial nonlinearity, especially at 1 atm. Over the range of pressures between 1 and 10 atm, the magnitude of the slope of voltage vs. current density traces decreases with increasing pressure. The greatest change was observed between 1 and 3 atm. with a modest change between 3 and 10 atm. Between 10 and 15 atm, no significant change was observed over the linear portion (for current densities ≤ 300 mA/cm^2). A plot of the slope vs. 1/pressure could be adequately described by

$$R_{Cell} \approx 0.5 + \frac{0.11}{P} \ \Omega cm^2 \qquad (9)$$

Note that the slope is 3 to 4 times that for electrolyte-supported cells and about half of that for cathode-supported cells estimated here for parameters given in Figure #2. In view of the differences in porosities and possible effects related to pore morphology, exact correspondence is not to be expected. Nevertheless, it is interesting to note that indeed there is an effect of concentration polarization and its dependence on pressure. Also, the fact that the intercept for the Westinghouse cell is 0.5 Ωcm^2 shows that the cell resistance is inherently high, possibly due to the cell design (long current path) or possible effects of charge transfer resistance. The reason the observed effect of pressure, although greater than expected based on Nernst potential, is modest compared to calculations is the inherently high cell resistance.

Similar calculations as above have also been performed on anode-supported cells. The results show that in this case also there is a significant contribution of concentration polarization with the result that under a high pressure operation, the concentration polarization effects are drastically reduced.

Theoretical Analysis of the Effect of Pressure: Activation Polarization: Finally, a comment is in order regarding the expected dependence of activation polarization on total pressure. Although the dominant effect of pressure is to lower the concentration polarization, there is also another beneficial effect of pressure; which is to lower the activation polarization or the charge transfer resistance. Recent theoretical analysis [13] has shown that porous composite electrodes can be designed to lower the overall charge transfer resistance. For a porous electrode, it has been shown that [13]

$$R_{ct}^{eff} \approx \sqrt{\frac{R_{ct} d}{\sigma(1-V_v)}} \qquad (10)$$

where R_{ct}^{eff}, d, V_v, and σ are respectively effective charge transfer resistance of a porous composite electrode, grain size of YSZ in the electrode, porosity of the electrode, and ionic conductivity of YSZ in the electrode; and R_{ct} is the intrinsic charge transfer resistance between the electrode material (e.g. LSM) and the electrolyte (YSZ). This latter quantity depends upon a number of factors such as the particle size of the electrode material (e.g. LSM), three phase boundary (TPB) length, electronic properties of the electrode material, and the degree of gas adsorption at TPB. The degree of gas adsorption is directly proportional to the partial pressure of the species of interest, e.g. oxygen [14]. The higher the degree of adsorption, the lower is the R_{ct}. That is, R_{ct} is inversely proportional to the gas pressure. Thus, it is expected that activation overpotential must also decrease with increased pressure, an added benefit for application in hybrid systems.

IV. SUMMARY

The preceding calculations show that concentration polarization decreases with increasing pressure and thus improves the cell performance in cathode-supported and anode-supported cells in which a relatively thick porous electrode (cathode or anode) exhibits a significant concentration polarization at low pressures. This is not the case in electrolyte-supported cells as the electrodes are thin in such a case. From a design standpoint, it is imperative that either one of the electrodes is thick enough to serve as the support structure or the electrolyte be the support structure. The present work shows that one should use either cathode-supported or anode-supported, but not electrolyte-supported cells in order to realize the potentially enormous improvement in performance at high pressures. This is especially important for hybrid applications (SOFC in combination with a gas turbine).

Acknowledgments: The work at the University of Utah was supported by Gas Research Institute and the State of Utah under its Centers of Excellence Program. The pressurized SOFC effort at Westinghouse is supported by Ontario Hydro and its Canadian funding partners, and New Energy Development Organization (NEDO) of Japan and its participating electric power companies.

REFERENCES

1) A. McDougall, 'Fuel Cells', The MacMillan Press, London, (1976).
2) M. Williams, in '1996 Fuel Cell Seminar', p.1, Orlando, FL, November, (1996).
3) S. C. Singhal, in Proceedings of the Fifth International Symposium on Solid Oxide Fuel Cells (SOFC-V), edited by U. Stimming, S. C. Singhal, H. Tagawa, and W. Lennert, The Electrochemical Soc., Pennington, NJ, (1997).
4) S. C. Singhal, in '1996 Fuel Cell Seminar', p.28, Orlando, FL, November (1996).
5) S. E. Veyo and W. Lundberg, in '1996 Fuel Cell Seminar', p.776, Orlando, FL, November, (1996).
6) A. V. Virkar and K. Z. Fung, unpublished work, (1996).
7) E. A. Mason and A. P. Malinauskas, 'Gas Transport in Porous Media: The Dusty Gas Model', Elsevier, Asmterdam, (1983).

8) E. L. Cussler, 'Diffusion: Mass Transfer in Fluid Systems', Cambridge University Press, London, (1995).
9) K. Z. Fung and A. V. Virkar, in Proceedings of the Fourth International Symposium on Solid Oxide Fuel Cells, edited by M. Dokiya, O. Yamamoto, H. Tagawa, and S. C. Singhal, The Electrochemical Society publication, p.1105, (1995).
10) M. Hsu, D. Nathanson, D. T. Bradshaw, D. R. Stephenson, and R. Goldstein, in '1996 Fuel Cell Seminar', p.183, Orlando, FL, November (1996).
11) R. Privette, M. A. Perna, K. Kneidel, J. Hartvigsen, S. Elangovan, and A. Khandkar, in '1996 Fuel Cell Seminar', p.206, Orlando, FL, November (1996).
12) R. C. Ruhl, M. A. Petrick, and T. L. Cable, in '1996 Fuel Cell Seminar', p.187, Orlando, FL, November (1996).
13) C. W. Tanner, K. Z. Fung, and A. V. Virkar, *J. Electrochem. Soc.*, **144** [1] 21-30 (1997).
14) A. W. Adamson, 'Physical Chemistry of Surfaces', John Wiley & Sons, New York, (1976).

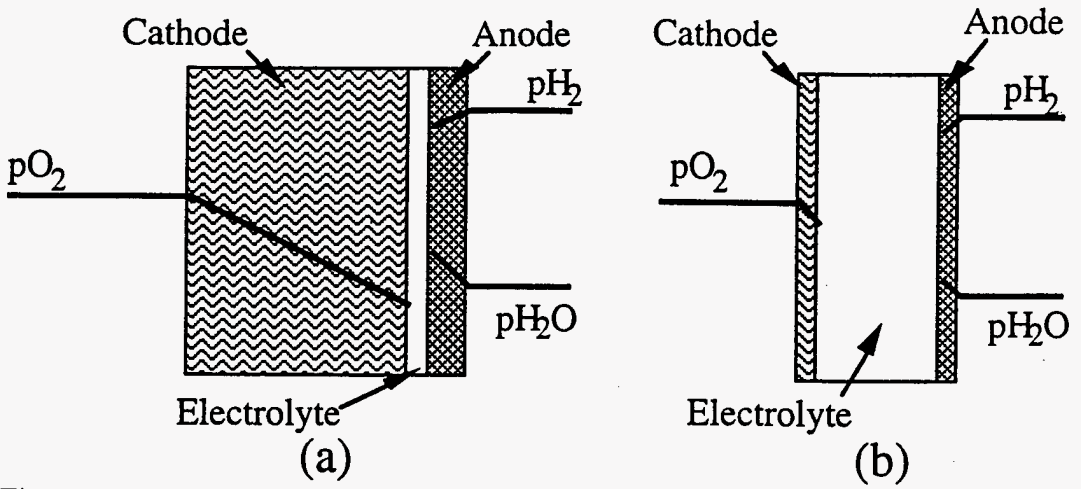

Figure #1: Schematics showing cathode-supported (a), and electrolyte-supported (b) cells. Also shown are expected variations in the partial pressures of oxygen, hydrogen, and water vapor. In the cathode-supported cells, substantial concentration polarization is expected on the cathodic side. In the electrolyte-supported cells, the main contribution to the cell resistance is the ohmic contribution of the electrolyte.

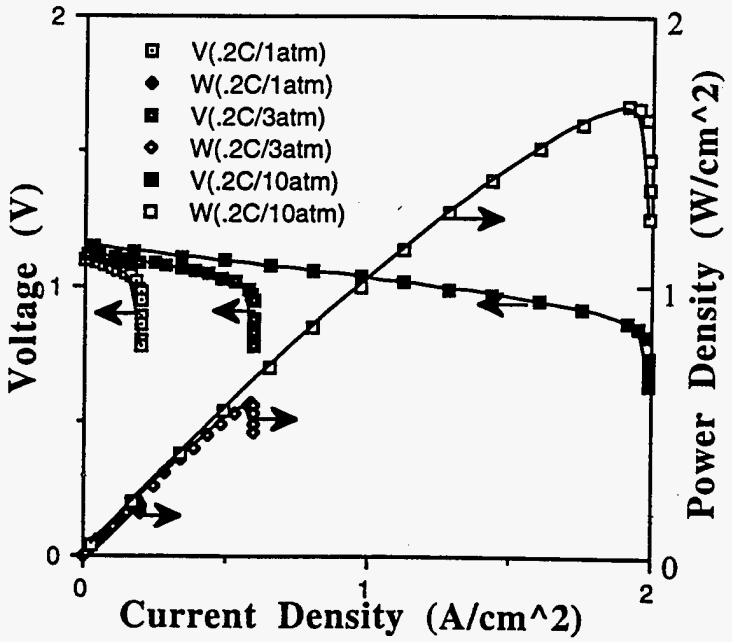

Figure #2: Theoretically calculated effect of total pressure on the performance of cathode-supported SOFCs: The figure shows voltage and power density vs. current density traces calculated for 1, 3, and 10 atm. pressure at 800°C. The cell dimensions are as follows: Cathode thickness = 2 mm, anode thickness = 25 μm, and electrolyte (YSZ) thickness = 20 μm. The legend .2C in the figure denotes cathode thickness.

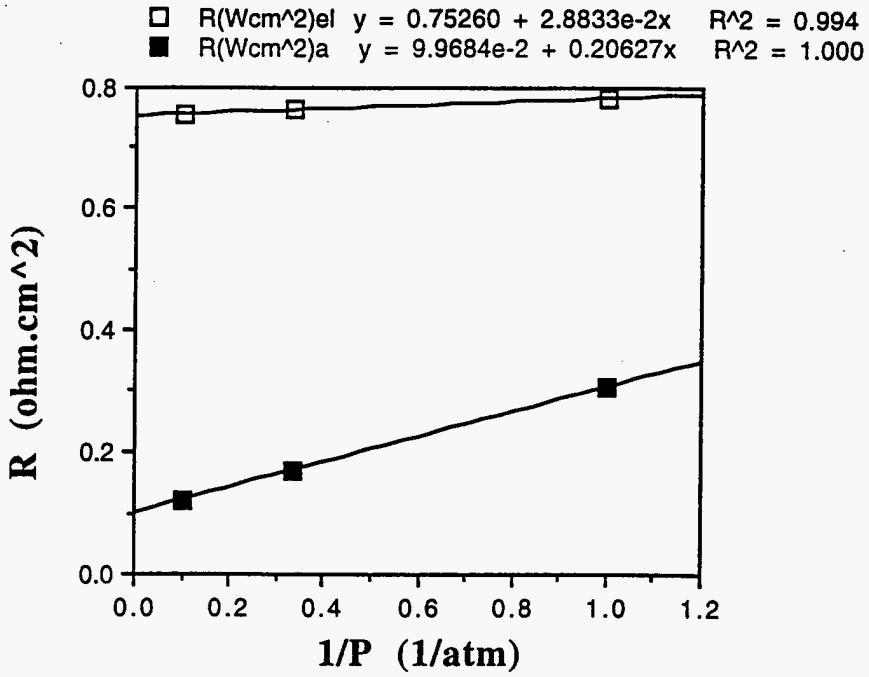

Figure #3: Plot of the calculated cell resistance, inclusive of concentration polarization, vs. 1/pressure, for cathode-supported and electrolyte-supported cells. The slope of the plot is a measure of the effect of pressure on concentration polarization.

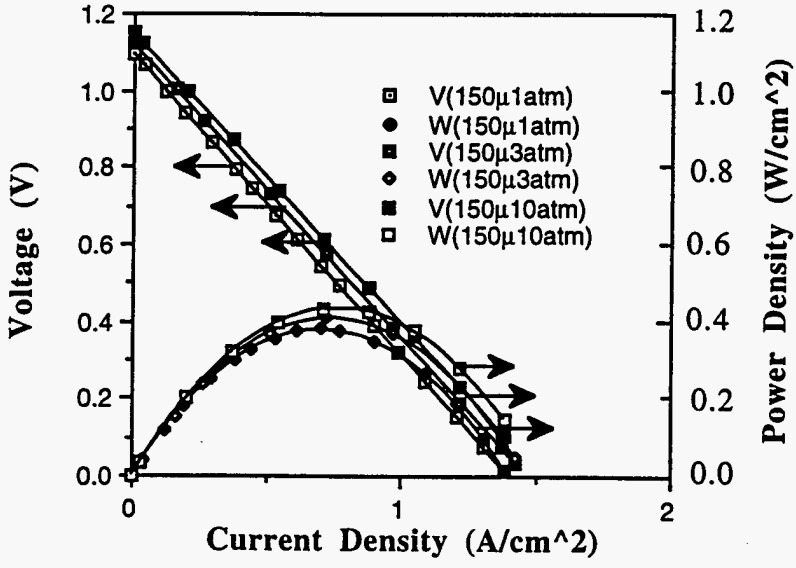

Figure #4: Theoretically calculated effect of total pressure on the performance of electrolyte-supported SOFCs: The figure shows voltage and power density vs. current density traces calculated for 1, 3, and 10 atm. pressure at 800°C. The cell dimensions are as follows: Cathode thickness = 25 µm, anode thickness = 25 µm, and electrolyte (YSZ) thickness = 150 µm. The highest power density calculated is about 0.45 W/cm^2 compared to ~1.6 W/cm^2 for cathode-supported cells.

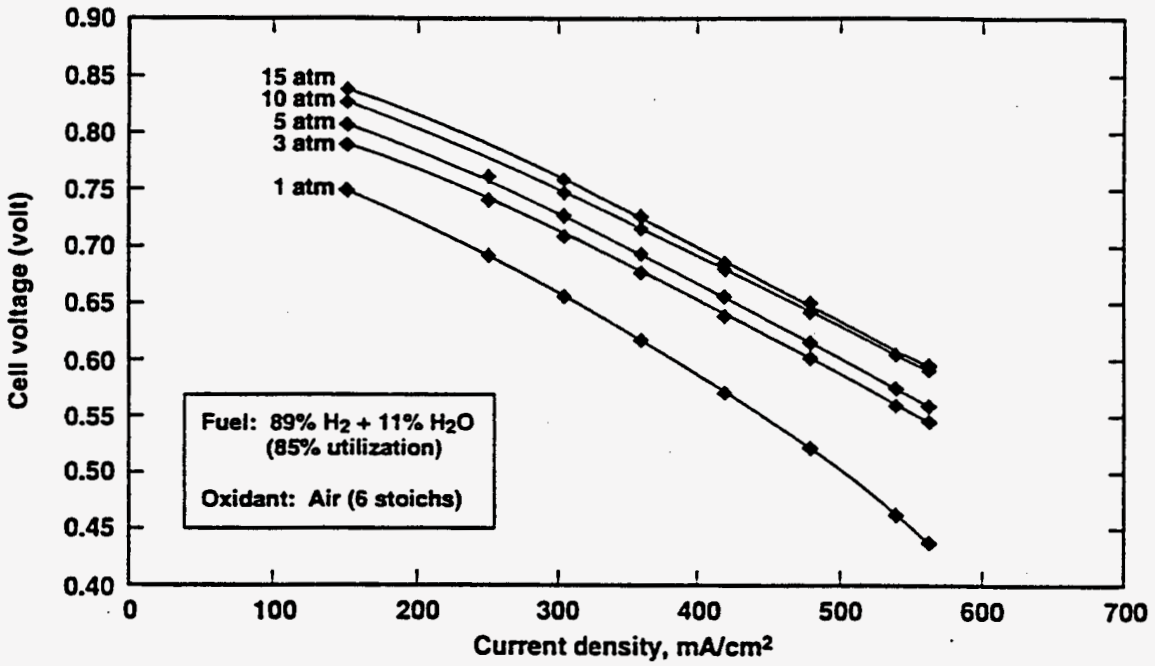

Figure #5: Experimentally measured effect of pressure on cell performance [3].

Report Number (14) DOE/FETC/C--98/7303
CONF-9706417[illegible]6--

Publ. Date (11) 199712
Sponsor Code (18) DOE/FE, XF
JC Category (19) UC-101, DOE/ER

DOE